**Proceedings of the ASME 2021 30th Conference on Information Storage and Processing Systems**
**ISPS2021**
**June 2-3, 2021, Virtual, Online**

# ISPS2021-65257

# DESIGN OF A 2 DOF SHAPE MEMORY ALLOY ACTUATOR USING SMA SPRINGS

**Hussein F. M. Ali**[1,2]
[1]Mechanical Engineering, Benha University, Benha, Egypt

**Youngshik Kim**[2]
[2]Mechanical Engineering, Hanbat National University Daejeon, Korea

## ABSTRACT

*In this paper, we developed two degree of freedom shape memory alloy (SMA) actuator using SMA springs. This module can be applied easily to various applications: device holder, artificial finger, grippes, fish robot, and many other biologically inspired applications, where small size and small wight of the actuator are very critical. This actuator is composed of two sets of SMA springs: one set is for the rotation around the X axis (roll angle) and the other set is for the rotation around the Y axis (pitch angle). Each set contains two elements: one SMA spring and one antagonistic SMA spring. We used an inertia sensor (IMU) and two potentiometers for angles feedback.*

*The SMA actuator system is modeled mathematically and then tested experimentally in open-loop and closed-loop control. We designed and experimentally tuned a proportional integrator derivative (PID) controller to follow the set points and to track the desired trajectories. The main goal of the presented controller is to control roll and pitch angles simultaneously in order to satisfy set points and trajectories within the work space. The experimental results show that the two degree of freedom SMA actuator system follows the desired setpoints with acceptable rise time and overshoot.*

**Keywords:** Shape memory alloy, 2-DOF actuator, Soft robot, PID control, trajectory tracking.

## 1. INTRODUCTION

Multiple degrees of freedom actuators are very useful in various applications where compliance, and compact size are significantly impact the cost and performance.

Recently, the utilization of smart materials in various biomedical applications has increased significantly. One group of these materials is the Shape Memory Alloys (SMAs). The advantages of SMAs include noiseless actuation, compact size, high force to weight ratio, and high-density work. The SMA's flexibility makes it possible to develop various configuration shapes, which allows adaption to many applications [1,2]. For instance, Four SMA springs are used for two-DOF robotic module [3, 4] and three SMA springs are used to build modular unit and then six modules are used to build Multi-DOF robot [5].

To study the system dynamics and to develop a closed-loop control of the SMA actuator efficiently, we need to model the dynamics of SMA. There have been different methods to model the dynamics of SMA wire and SMA spring [6-11].

In previous research [12-13], we fabricated and modeled a SMA finger considering the tensile stress induced in SMA wire when heated and applied PD controller.

In this research we develop a two-DOF actuator using four SMA springs. Its mathematical model is presented considering shear stress. We tune the PID controller using IMU sensor feedback experimentally.

This paper is organized as follows: The two-DOF actuator unit and the mechanical characterization of the SMA spring are described in section 2. The mathematical model is then derived and the controller architecture is explained in section 3. Finally, the experimental results are discussed in section 4.

## 2. Two-DOF ACTUATION UNIT

This actuator is composed of two sets of SMA springs, as shown in Fig.1: one set is for the rotation around the X axis (roll angle) and the other set is for the rotation around the Y axis (pitch angle). The X axis set contains two elements: one SMA spring (SMA1) and one antagonistic SMA spring (SMA2). The Y axis set contains two elements: one SMA spring (SMA3) and one antagonistic SMA spring (SMA4). We used an inertia sensor (IMU) and two potentiometers for the two angles feedback.

### 2.1 SMA actuator mechanical characterization

This section presents the mechanical characterization of the SMA spring unit; especially, the spring constants, and the

[1] Emails: hussein.ali@ejust.edu.eg,
[2] Corresponding author: youngshik@hanbat.ac.kr

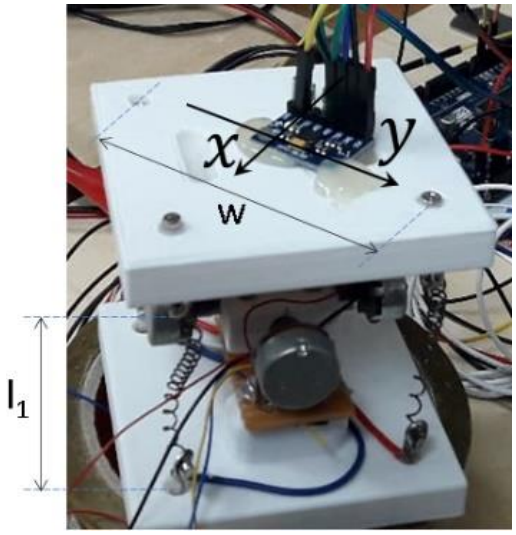


**Fig.1:** 2-DOF SMA actuator

mechanical responses at various temperature conditions 25ºC, 40ºC, 70ºC, and 90ºC. Where the SMA spring has: wire diameter d= 0.51 mm; spring outer diameter $D_{out}$=3.45 mm; Number of coils n=10 turns. The spring constant of the SMA spring is investigated while increasing and decreasing the elongation.

Fig.2 shows the test rig used in the mechanical characterization of the SMA spring. SMA spring module (1) is clamped with the bench vise. As an input, the force sensor (2), (3Kg range, Model: BCL-3L) and the amplifier (Model: LCT-II). Then the other side is held to a moving part 2 mm step by step (3), which connected to power screw then a stepper motor (4) which has driver (5) and is controlled by Arduino due (6) to do some tests one of them is the mechanical characterization of the SMA actuator. The force reading is amplified through transducer amplifier LCT-II and acquired using the Data acquisition NI USB-6009 (7). The Force versus elongation correlation is shown in Fig.3. where elongation is x axis and force is the y axis and $R^2$ is the correlation.

At 70ºC, y = 0.3377x + 0.6169, $R^2$ = 0.99, while increasing $\Delta l$

y = 0.3748x - 1.6855, $R^2$ = 0.98, while decreasing $\Delta l$

At 90ºC, y = 0.466x + 0.9277, $R^2$ = 0.99, while increasing $\Delta l$

y = 0.484x - 1.2673, $R^2$ = 0.98, while decreasing $\Delta l$

At 70ºC, the force can reach 11.46 N at displacement 32 mm

At 90ºC, the force can reach 15.4 N at displacement 32 mm

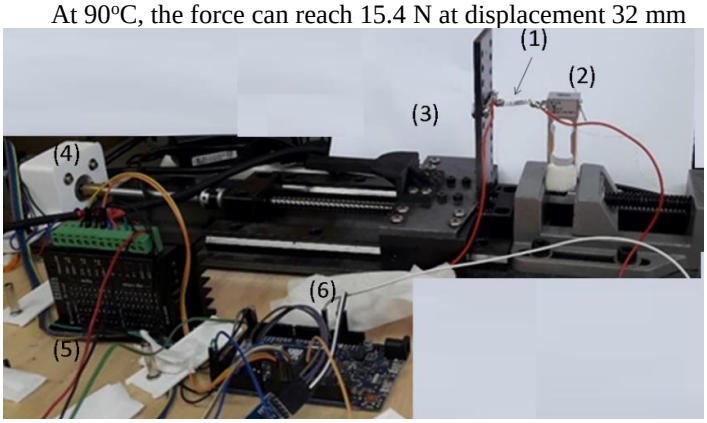


**Fig.2:** Test rig for SMA actuator mechanical characterization.

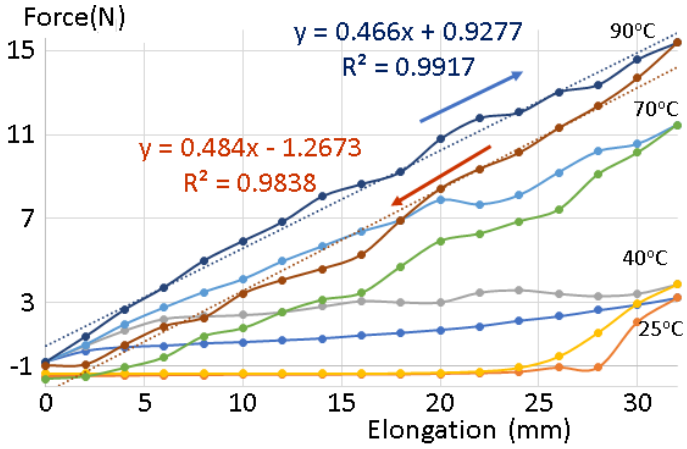


**Fig.3:** Spring constants of the SMA actuator.

At 70ºC, the spring constant is 337.7 N/m when the elongation $\Delta l$ is increasing and the spring constant is 374.8 N/m when it is decreasing. At 90ºC, the spring constant is 466 N/m when the elongation $\Delta l$ is increasing and the spring constant is 484 N/m when it is decreasing.

## 3. MATHEMATICAL MODELING

### 3.1 Kinematic Mathematical Modeling

Roll and pitch angles can be calculated based on the geometrical constrains as shown in figure 1.a.

if SMA1 is active: $\theta_x = \sin^{-1}\left(\frac{\Delta l_1}{w/2}\right)$ .....(1)

if SMA2 is active: $\theta_x = \sin^{-1}\left(\frac{\Delta l_2}{w/2}\right)$ .....(2)

If both SMA1 and SMA2 are active, then $\Delta l_1 = \Delta l_2$

if SMA3 is active: $\theta_y = \sin^{-1}\left(\frac{\Delta l_3}{w/2}\right)$ .....(3)

if SMA4 is active: $\theta_y = \sin^{-1}\left(\frac{\Delta l_4}{w/2}\right)$ .....(4)

If both SMA3 and SMA4 are active then $\Delta l_3 = \Delta l_4$

Where $\Delta l_i$ is the change of the length of the SMA spring number i; w is the diagonal length. (i=1,2,3, and 4).

### 3.2 SMA Mathematical Modeling

The length of the SMA spring is dependent on the applied electrical energy (current and voltage) and the loading force (shear stress). All SMA Parameters are given in Table1. The SMA spring constitutive model of is based on Hisaaki model [6], and Elahinia model [9]. This model can be described as a time derivative relation between torsional stress $\tau$, temperature $T$, shear strain $\gamma$ and martensite fraction $\xi$ as

$\tau^{\cdot} = G\gamma^{\cdot} + \Omega\xi^{\cdot} + \Theta T^{\cdot}$ .....(5)

where, $G$ is shear modulus, $\Omega$ is a transformation tensor and $\Theta$ is a thermoelastic tensor.

The martensite fraction $\xi$ from martensite state to austenite state shows hysteresis phenomenon. Note $\xi$ = 1 implies that SMA is in martensite state (cold), and $\xi$ = 0 means that SMA is completely in austenite state (hot) state. This conversion (from martensite to austenite state) produce stress in SMAs. This conversion is a combination of loading ($\tau^{\cdot}$) and heating ($T^{\cdot}$) and can be represented as:

$\xi^{\cdot} = \xi_T(T,\tau)T^{\cdot} + \xi_\tau(T,\tau)\tau^{\cdot}$ .....(6)

where $\xi_T, \xi_\tau$ are dependent on the temperature and shear stress

**Table 1:** Flexinol (NiTi) SMA Parameters

| Parameter | Definition | Value | Unit |
|---|---|---|---|
| $M_s$ | Martensite start temperature | 72 | °C |
| $M_f$ | Martensite final temperature | 62 | °C |
| $A_s$ | Austenite start temperature | 88 | °C |
| $A_f$ | Austenite final temperature | 98 | °C |
| $C_A$ | Austenite stress-influence coefficient | 10 | MPa °C$^{-1}$ |
| $C_M$ | Martensite stress-influence coefficient | 10 | MPa °C$^{-1}$ |
| $E_A$ | Austenite Young modulus | 75 | GPa |
| $E_M$ | Martensite Young modulus | 28 | GPa |
| $R_A$ | Austenite wire resistance | 100 | μΩ cm |
| $R_M$ | Martensite wire resistance | 80 | μΩ cm |
| $\Theta_A$ | Austenite thermal expansion coefficient | 11 | μ Pa °C$^{-1}$ |
| $\Theta_M$ | Martensite thermal expansion coefficient | 6.6 | μPa °C$^{-1}$ |
| $\sigma_s^{cr}$ | Detwinning start stress | 25 | MPa |
| $\sigma_f^{cr}$ | Detwinning finish stress | 78 | MPa |
| $\varepsilon_L$ | Maximum recoverable strain | 4.1 | % |
| $D$ | SMA wire diameter | 0.254 | mm |
| $C_p$ | Thermal capacity of SMA wire | 2.046 | MJ m$^{-3}$ °C |

If ( $(A_s < T_A < T_f)$ *and* $(\dot{T_A} > 0)$ )

$$\xi_T(T,\tau) = \frac{-\xi_M a_A}{2}\sin\left(a_A(T_A - A_s)\right)$$

$$\xi_\tau(T,\tau) = \frac{-\xi_M b_A}{2}\sin\left(a_A(T_A - A_s)\right) \quad \ldots\ldots\ldots\ldots\ldots (7)$$

If ( $(M_f < T_M < M_s)$ *and* $(\dot{T_M} < 0)$ )

$$\xi_T(T,\tau) = \frac{(1-\xi_A)a_M}{2}\sin\left(a_M(T_M - M_f)\right)$$

$$\xi_\tau(T,\tau) = \frac{(1-\xi_A)b_M}{2}\sin\left(a_M(T_M - M_f)\right) \quad \ldots\ldots. (8)$$

Otherwise $\xi_T(T,\tau) = 0$; $\xi_\tau(T,\tau) = 0$ …… (9)

where: $a_A := \frac{\pi}{(A_f - A_s)}$, $a_M := \frac{\pi}{(M_s - M_f)}$, $T_A = T - \frac{\tau}{C_A}$

$b_A := \frac{-a_A}{C_A}$, $b_M := \frac{-a_M}{C_M}$, $T_M = T - \frac{\tau}{C_M}$

The longitudinal force F produced by a shape memory alloy spring is modeled by considering a helical spring with the diameter D, n coils and the wire diameter d. It is assumed that the force, F, is resisted by the torsional shear stress developed on the circular cross section of the helical shaped wire [11] Therefore, the equilibrium can be written as follows:

$$F = \frac{4\pi}{D}\int_0^{d/2} \tau r^2 dr \quad \ldots\ldots\ldots\ldots\ldots\ldots\ldots\ldots\ldots\ldots\ldots\ldots\ldots\ldots\ldots\ldots (10)$$

where r is the radial coordinate through its wire cross section. The shear strain, γ, is assumed to be linearly distributed through the wire cross section (γ varies from zero, at the center, to a maximum value $\gamma_{max}$, at the surface of the wire), from which follows the kinematics relation:

$$\gamma(r) = \frac{r}{d/2}\gamma_{max} \quad \ldots\ldots\ldots\ldots\ldots\ldots\ldots\ldots\ldots\ldots\ldots\ldots\ldots\ldots (11)$$

$$\gamma_{max} = \frac{d}{\pi D^2 n}u \quad \ldots\ldots\ldots\ldots\ldots\ldots\ldots\ldots\ldots\ldots\ldots\ldots\ldots\ldots\ldots\ldots (12)$$

where u is the longitudinal spring displacement.

### 3.3 Heat transfer mathematical model

In the heat transfer model, the rate of change of temperature in degree Celsius per second:

$$\dot{T} = \frac{iv - h_c A_c (T - T_a)}{m_w C_p} \quad \ldots\ldots\ldots\ldots\ldots\ldots\ldots\ldots\ldots\ldots\ldots\ldots\ldots\ldots (13)$$

Where $C_p$ represents the specific heat constant; $m_w$ is the mass of the SMA spring; $i, v$ are the applied electrical current and voltage; $T_a$ is the ambient temperature.

$$h_c = h_0 + h_2 T^2$$

$$h_0 = 120\,, h_2 = 0.001$$

$$L = \pi D n, \qquad A_c = \pi d L$$

where d is wire diameter, D mean diameter of the spring, L is wire length used in building the spring, n is the number of coils.

### 3.4 Series Elastic Actuator model

$$I_{xx}\ddot{\theta_x} + c\dot{\theta_x} = (F_1 - F_2)w/2 \quad \ldots\ldots\ldots\ldots\ldots\ldots\ldots\ldots\ldots\ldots\ldots\ldots (14)$$

$$I_{yy}\ddot{\theta_y} + c\dot{\theta_y} = (F_3 - F_4)w/2 \quad \ldots\ldots\ldots\ldots\ldots\ldots\ldots\ldots\ldots\ldots\ldots\ldots (15)$$

where $I_{xx}$ is the moment of inertia around the joint axis x, $I_{yy}$ is the moment of inertia around the joint axis y, c is the damping coefficient, and w is the diagonal length of the end effector as shown in Fig.1.

### 3.5 PID Control

The control algorithm contains two PID controllers. One for each angle $\theta_x$ and $\theta_y$ as shown in Fig.4.

$$e_x = \theta_x - \theta_{xsp} \quad \ldots\ldots\ldots\ldots\ldots\ldots\ldots\ldots\ldots\ldots\ldots\ldots\ldots\ldots\ldots\ldots (16)$$

$$C_x = K_p e_x + K_i \int e_x\, dt + K_d \frac{de_x}{dt} \quad \ldots\ldots\ldots\ldots\ldots\ldots\ldots\ldots\ldots\ldots\ldots\ldots\ldots\ldots (17)$$

$$e_Y = \theta_Y - \theta_{ysp} \quad \ldots\ldots\ldots\ldots\ldots\ldots\ldots\ldots\ldots\ldots\ldots\ldots\ldots\ldots\ldots\ldots (18)$$

$$C_y = K_p e_x + K_i \int e_x\, dt + K_d \frac{de_x}{dt} \quad \ldots\ldots\ldots\ldots\ldots\ldots\ldots\ldots\ldots\ldots\ldots\ldots\ldots\ldots (19)$$

where $\theta_{xsp}$ and $\theta_{ysp}$ are the desired set points, $e_x$ and $e_y$ are the errors, $K_p, K_i, K_d$ are the PID controller gains, $C_x$, $C_y$ are the control signals. Then the PWM control input is applied to control the corresponding SMA spring. For positive $C_x$, the SMA1 is actuated and the SMA2 is actuated for negative $C_x$. Similarly, for positive $C_y$, the SMA3 is actuated and the SMA4 is actuated for negative $C_y$.

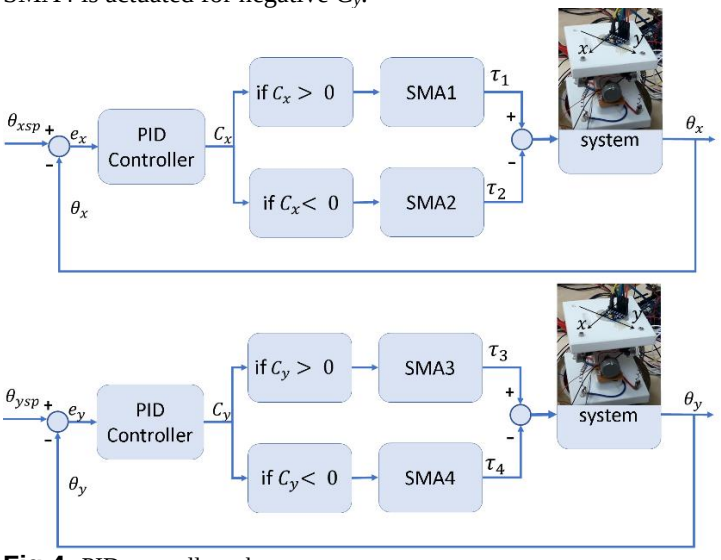


**Fig.4:** PID controller scheme

## 4. RESULTS AND DISCUSSION

By trial and error, the controller gains are tuned experimentally to be $K_p = 5,\ K_i = 0.01,\ K_d = 0.7$. The experimental setup for the control experiments is shown in Fig.5. To test the controller, we applied a square wave trajectory between 0° ,10°, -10°. The performance measures are the delay time, rise time and the overshoot percentage; where the delay time is the time from a command start until its effect starts. The rise time is the time from the command start until it reaches 100% of the setpoint. Overshoot is the ratio between the maximum value and the setpoint. In experiment 1, Fig.6 shows the roll angle response to a square trajectory. In experiment 2, Fig.7 pitch angle response to a square trajectory. Table2 shows the performance measures of the two experiments, where input voltage: 4 volt, the max current: 4 Amp. In experiment 3, Fig.8 shows trajectory tracking results applying square waves for the roll angle and pitch angle. Input voltage:4 volt, Max current:4.7 Amp

**Table 2:** Performance measures

| Experiment | Delay time (sec) | Rise time (sec) | Overshoot % |
|---|---|---|---|
| Exp.1, Fig.6 | 0.66<br>0.58<br>0.4 | 1.3<br>(2.18) 1.09<br>1.3 | 14%<br>3%<br>7% |
| Exp.2, Fig.7 | 0.55<br>0.47<br>0.4 | 1.26<br>(1.8) 1.09<br>1.4 | 17.7%<br>5.5%<br>7% |

From these experiments we found that the PID controller succeeded to follow the trajectory with acceptable rise time and overshoot. Moreover, we found also that the preheating reduces the delay time, rise time and overshoot significantly. Additional videos are in the supplementary section.

## CONCLUSION

We developed two degree of freedom actuator which can adjust the end effector's orientation (roll and pitch) using SMA springs. PID controllers for the actuator are tuned and tested experimentally. The delay time can be as minimum as 0.4 sec. And the rise time can be as minimum as 0.9 sec. While the overshoot can be as minimum as 3%. From these experiments we found that the preheating reduces the delay time, rise time and overshoot significantly.


## ACKNOWLEDGEMENTS

This work was supported by the National Research Foundation of Korea (NRF) grant funded by the Korea Government (MSIT) (No. 2017R1A2B4008056).

Also, the first author is funded by the Korea Research Fellowship (KRF) program by the National Research Foundation (NRF) with KRF Grant (2019H1D3A1A01071124).


## SUPPLEMENTARY MATERIAL

https://youtu.be/nYgkMxbvmh8 -> the actuator as mobile holder
https://youtu.be/ShZGA6Wff_c -> Control trajectory of $\theta_x$
https://youtu.be/bW54eUEdcpc-> Control trajectory of $\theta_y$
https://youtu.be/LqyZNxgaSFw -> Control trajectory of $\theta_x$and $\theta_y$

## REFERENCES


[1] J. M. Jani, M. Leary, A. Subic, and M. A. Gibson, "A review of shape memory alloy research, applications and opportunities," Materials & Design (1980-2015), vol. 56, pp. 1078–1113, 2014.


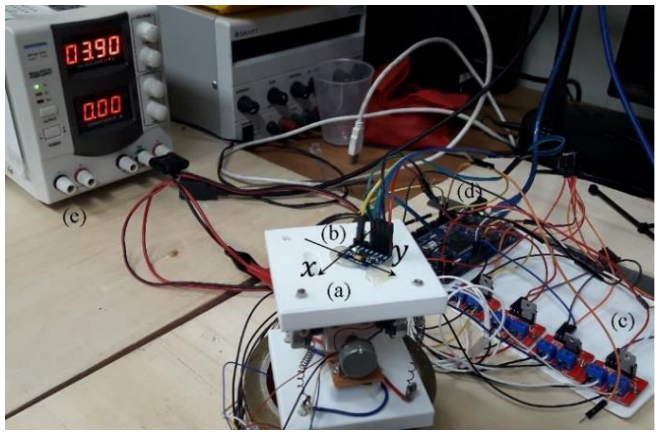


**Fig.5:** Experimental setup for controlling the 2DOF actuator (a) End effector (b) IMU sensor (c) Driver (d) Arduino due (e) Power supply

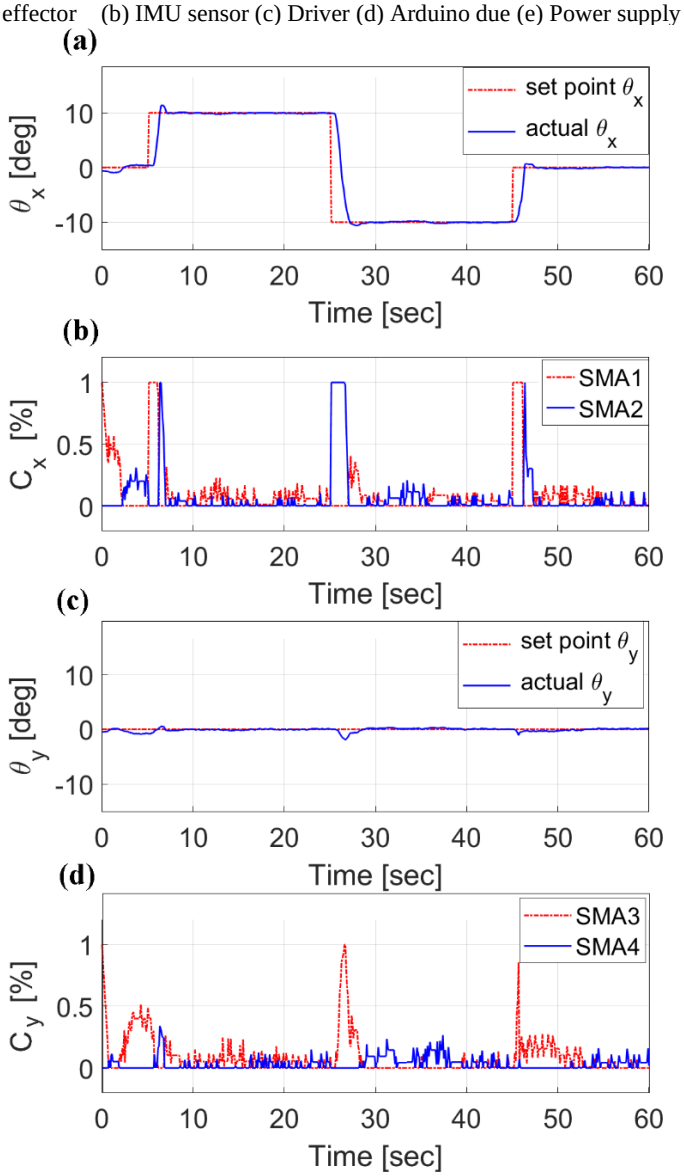


**Fig.6:** Control experiment applying a square wave for the desired roll trajectory while regulating the pitch angle. (a) roll angle $\theta_x$ (b) control signal $C_x$(c) pitch angle $\theta_y$ (d) control signal $C_y$

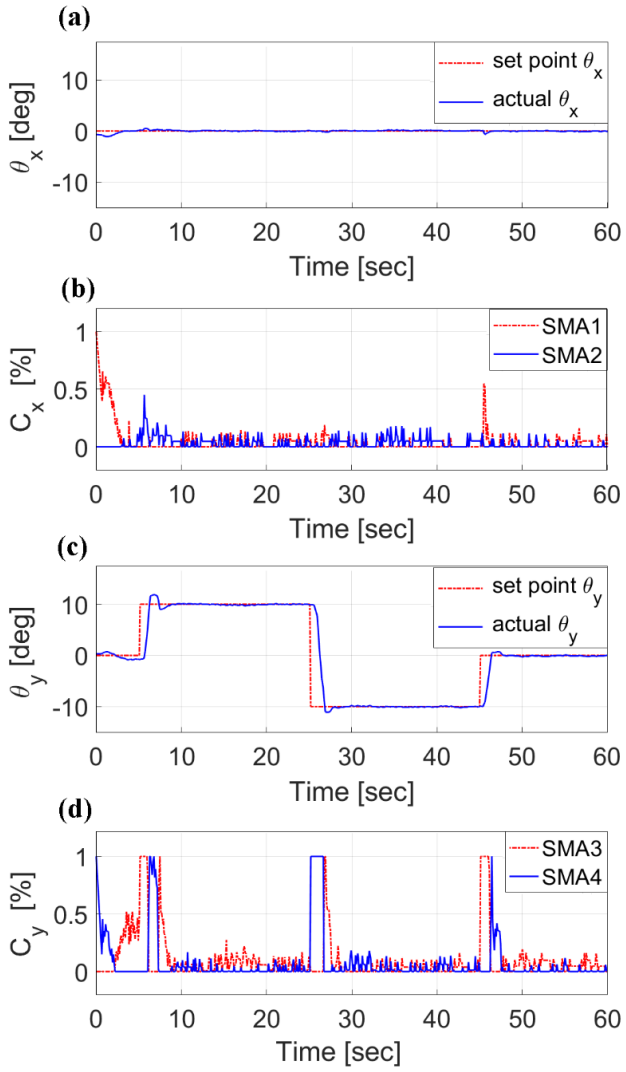


**Fig.7:** Control experiment applying a square wave for the desired pitch trajectory while regulating the roll angle. (a) roll angle $\theta_x$ (b) control signal $C_x$(c) pitch angle $\theta_y$ (d) control signal $C_y$

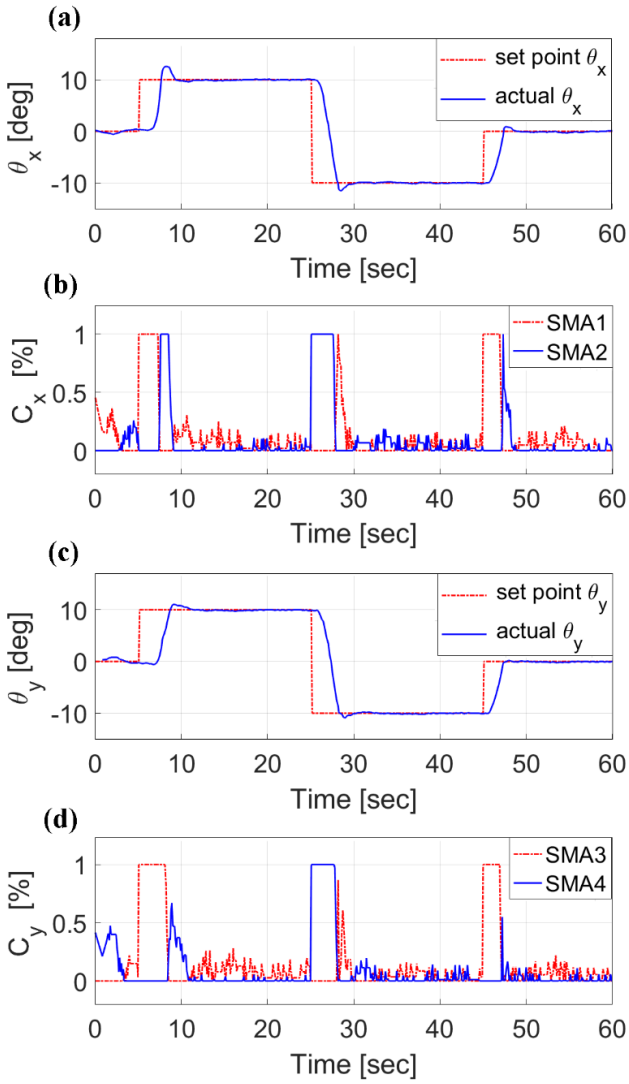


**Fig.8:** Trajectory tracking experiment applying square waves for desired roll and pitch angle trajectories. (a) roll angle $\theta_x$ (b) control signal $C_x$(c) pitch angle $\theta_y$ (d) control signal $C_y$


[2] J.-H. Lee, Y. S. Chung, and H. Rodrigue, “Long shape memory alloy tendon-based soft robotic actuators and implementation as a soft gripper,” Scientific reports, vol. 9, pp. 1–12, 2019.

[3] Hadi A, Yousefi-Koma A, Moghaddam MM, Elahinia M, Ghazavi A., "Developing a novel SMA-actuated robotic module." Sensors and Actuators A: Physical 162.1,2010.

[4] Sheikhi, M. M., A. Hadi, and M. Ghasemi Varzaneh. "Design of a basic module for angular motion of spherical joints using the actuators of shape memory alloys and magnetic stabilization system." Modares Mech. Eng. 19.2, 2019.

[5] Cheng, Changxi, Jianxiang Cheng, and Wenkai Huang. "Design and development of a novel SMA actuated multi-DOF soft robot." IEEE Access 7 (2019).

[6] K. Tanaka, “A thermomechanical sketch of shape memory effect: one-dimensional tensile behavior,” 1986.

[7] C. Liang and C. A. Rogers, “One-dimensional thermomechanical constitutive relations for shape memory materials,” Journal of int. mat. sys. & str., vol. 8, no. 4, 1997.

[8] L. C. Brinson, “One-dimensional constitutive behavior of shape memory alloys: thermomechanical derivation with non-constant material functions and redefined martensite internal variable,” Journal of int. mat. sys. & str., vol. 4, 1993.

[9] M. H. Elahinia and M. Ahmadian, “An enhanced sma phenomenological model: I. the shortcomings of the existing models,” Smart materials and structures, vol. 14, 2005.

[10] Tobushi, Hisaaki, and Kikuaki Tanaka. "Deformation of a shape memory alloy helical spring: Analysis based on stress-strain-temperature relation." JSME international journal. Ser. 1, Solid mechanics, strength of materials 34.1 (1991): 83-89.

[11] Aguiar, Ricardo AA, Marcelo A. Savi, and Pedro MCL Pacheco. "Experimental and numerical investigations of shape memory alloy helical springs." Smart Mat. and Str. 2010.

[12] Hussein F. M. Ali, H. Baek, T. Jang, Y. Kim, "Finger-Like Mechanism Using Bending Shape Memory Alloys", ASME Int. Conf. Information Storage and Processing Systems, ISPS2020, June 25-26, 2020, Milpitas, USA. 2020.

[13] Hussein F. M. Ali, A. Khan, H. Baek, B.Shin, Y. Kim, " Modeling And Control of A Finger-Like Mechanism Using Bending Shape Memory Alloys", Journal of MITE. 2021.